Disclosure of Discrete Sites for Phospholipid and Sterols at the Protein−Lipid Interface in Native Acetylcholine Receptor-Rich Membrane†

S. S. Antollini and F. J. Barrantes*

Instituto de Investigaciones Bioquímicas de Bahía Blanca, 8000 Bahía Blanca, Argentina

Received April 13, 1998; Revised Manuscript Received July 13, 1998

ABSTRACT: There is an increasing body of evidence to support the notion that the function of the nicotinic acetylcholine receptor (AChR) is influenced by its lipid microenvironment [see Barrantes, F. J. (1993) *FASEB J. 7*, 1460−1467]. We have recently made use of the so-called generalized polarization (GP) of the fluorescent probe Laurdan (6-dodecanoyl-2-(dimethylamino)naphthalene) to learn about the physical state of the lipids in *Torpedo marmorata* AChR native membrane [Antollini, S. S., Soto, M. A., Bonini de Romanelli, I., Gutiérrez Merino, C., Sotomayor, P., and Barrantes, F. J. (1996) *Biophys. J. 70*, 1275−1284] and cells expressing endogenous or heterologous AChR [Zanello, L. P., Aztiria, E., Antollini, S., and Barrantes, F. J. (1996) *Biophys. J. 70*, 2155−2164]. In the present work, Laurdan GP was measured in *T. marmorata* native AChR membrane by direct excitation or under energy transfer conditions in the presence of exogenous lipids. GP was found to diminish in these two regions upon addition of oleic acid and dioleoylphosphatidylcholine and not to vary significantly upon addition of cholesterol hemisuccinate, indicating an increase in the polarity of the single, ordered-liquid lipid phase in the two former cases. Complementary information about the bulk lipid order was obtained from measurements of fluorescence anisotropy of DPH and two of its derivatives. The membrane order diminished in the presence of oleic acid and dioleoylphosphatidylcholine. The location of Laurdan was determined using the parallax method. Laurdan lies at ∼10 Å from the center of the bilayer, i.e., at depth of ∼5 Å from the lipid−water interface. Exogenous lipids modified the energy transfer efficiency from the intrinsic fluorescence to Laurdan. This strategy is introduced as a new analytic tool that discloses for the first time the occurrence of discrete and independent sites for phospholipids and sterols, respectively, both accessible to fatty acids, and presumably located at a shallow depth close to the phospholipid polar head region in the native AChR membrane.

The nicotinic acetylcholine receptor (AChR)[1] is an integral membrane protein deeply embedded in the postsynaptic region of muscle, electrocyte, and nerve cells. There is growing evidence to support the notion that the function of this paradigm rapid ligand-gated receptor is influenced by its lipid milieu (see reviews in refs *1* and *2*). The first-shell, lipid belt, or "annular" lipid region surrounding the AChR, as early described in its native membrane environment (*3*), has received particular attention as a possible candidate region where this effect is exerted. Jones and McNamee (*4*) also found that a second class of lipids, nonannular lipids, could be distinguished in addition to the annular lipid.

Among the physical properties of the AChR membrane studied so far, the so-called lipid order parameter has received particular attention (e.g., ref *5*). One of the AChR functional properties, the ability to permeate ions, has been shown to be sensitive—within a narrow range of values—to the bulk fluidity of the membrane as measured by in vitro experiments with AChR reconstituted into liposomes of various lipid compositions (*6*−*8*). Sunshine and McNamee (*9*) also studied the fluidity of the host liposomes by steady-state fluorescence anisotropy of the probe diphenylhexatriene (DPH) at a fixed temperature and showed that AChR channel activity is maintained either in low or high fluidity environments. These authors suggested that lipid composition rather than fluidity determines the gating function of the channel.

To explore in more detail the physical characteristics of the membrane in which the AChR is inserted and of the AChR annular lipid region in particular, we have used here the amphiphilic fluorescent probe Laurdan (6-dodecanoyl-2-(dimethylamino)naphthalene) (*10*) and three fluorescent probes sensitive to the lipid order. Laurdan possesses an exquisite sensitivity to the phase state of the membrane. The physical origin of Laurdan spectral properties resides in its capacity to sense the polarity and the molecular dynamics of dipoles in its environment due to the effect of dipolar relaxation processes (*11*, *12*). An advantage of measuring

† This work was supported by grants from the Universidad Nacional del Sur, the Argentinian Scientific Research Council (CONICET), the Commission of Scientific Research of the Province of Buenos Aires (CIC), and Autordras/British Council grant to F.J.B.

* To whom correspondence should be addressed.

[1] Abbreviations: AChR, nicotinic acetylcholine receptor; CHS, cholesterol hemisuccinate; cmc, critical micellar concentration; DOPC, 1,2-di(*cis*-9-octadecenoyl)-*sn*-glycerophosphocholine; DPH, 1,6-diphenyl-1,3,5-hexatriene; *E*, fluorescence energy transfer efficiency; FRET, fluorescence resonance energy transfer; GP, generalized polarization; 18:1, oleic acid; PA-DPH, 3-(*p*-(6-phenyl)-1,3,5-hexatrienyl)phenylpropionic acid; PC, phosphatidylcholine; *n*-SLPC: 1-palmitoyl-2-stearoyl-*n*-doxyl-*sn*-glycerophosphocholine (where *n* is the position of the nitroxide spin label); TMA-DPH, 1-(4-trimethylammoniumphenyl)-6-phenyl-1,3,5-hexatriene *p*-toluenesulfonate; Trp, tryptophan.

10.1021/bi9808215 CCC: $15.00
Published on Web 10/31/1998

membrane polarity with Laurdan is the possibility of obtaining dynamic information from steady-state measurements.

We have recently used Laurdan as a reporter of AChR membrane physical state and been able to differentiate between the bulk bilayer lipid and the AChR annular lipid (*13*). We have also shown that the so-called generalized polarization (GP) of Laurdan is a sensitive tool to measure the physical state of this membrane region and can be linearly correlated with channel gating kinetics of the receptor protein in living cells (*14*). In vivo studies still fall short of rendering the topological resolution afforded by fluorescence studies in solution with purified AChR-rich membranes. We have therefore used the latter experimental paradigm to further investigate this problem.

Laurdan GP values depend on the polarity and dynamics of the dipoles in the environment of the probe. The main dipoles sensed by Laurdan in the membrane are water molecules. When no relaxation occurs, high GP values result, indicative of low water content in the hydrophilic/hydrophobic interface region of the membrane. Thus, GP values depend on the extent of water penetration allowed by local membrane packing. In the present work, we have taken advantage of these spectroscopic properties of Laurdan in order to learn about the possible influence of fatty acids, phospholipid, and cholesterol on the physical state of the membrane in which the AChR protein is embedded. Complementary studies with DPH and two derivatives of this fluorescent probe were also conducted to investigate the possible occurrence of local heterogeneities in the bulk lipid order across the AChR membrane and their possible modification by exogenous lipids. We found a gradient of lipid order with a more fluid hydrocarbon interior (sensed by DPH) than the more superficial levels of the membrane (sensed by PA- and TMA-DPH). Oleic acid decreases membrane order, the more pronounced changes occurring deep in the fatty acyl chain region. Laurdan's vertical position in the membrane was determined by the parallax method of Chattopadhyay and London (*15*). Changes in the efficiency of the energy transfer from the protein emission to Laurdan brought about by addition of exogenous lipids reveal for the first time the presence of distinct sites for phospholipid and cholesterol in the native AChR membrane.

MATERIALS AND METHODS

Materials

Torpedo marmorata specimens were obtained either from the Roscoff marine station in France or from the Mediterranean coast off Alicante, Spain. The latter were kindly provided by Dr. J. M. González-Ros. Fish were transported by ground in sealed plastic bags containing seawater and oxygen. On arrival, they were killed by pithing, and the electric organs were dissected and stored at −70 °C until further use. Laurdan, TMA-DPH, and DPH-PA were purchased from Molecular Probes (Eugene, OR). Spin-labeled phosphatidylcholine (SLPC) derivatives (1-palmitoyl-2-stearoyl-*n*-doxyl-*sn*-glycerophosphocholine, where *n* is the position of the nitroxide spin label) were purchased from Avanti Polar Lipids. DPH and all other drugs were obtained from Sigma Chemical Co., St. Louis, MO.

Methods

Preparation of AChR-Rich Membranes. Membrane fragments rich in AChR were prepared from the electric tissue of *T. marmorata* as previously described (*16*). Typically, specific activities in the order of 1.2−1.8 nmol of α-bungarotoxin sites/mg of protein were obtained. The integrity of the membranes was studied in a previous work from our laboratory (*17*). For fluorescent measurements, AChR-rich membranes were resuspended in buffer A (20 mM HEPES buffer, 150 mM NaCl, and 0.25 mM $MgCl_2$, pH 7.4) to obtain 50 μg of protein/mL (0.2 μM). The OD of the membrane suspension was kept below 0.1 to minimize light scattering.

Oleic Acid (18:1), DioleoylPhosphatidylcholine (DOPC), and Cholesterol Hemisuccinate (CHS) Incorporation. The sodium salt of oleic acid was dissolved in buffer and sonicated. DOPC was prepared as multilamellar liposomes (evaporated under N_2, resuspended in buffer A, and sonicated until clarity). Oleic acid was added in aliquots to give final (nominal) concentrations <2.5 μM, i.e., well below the cmc of 18:1 (∼6 μM) (*18*). The partition coefficient of 18:1 in heptane:water is 1000 (*19*). CHS was dissolved in C:M (2:1), evaporated under N_2, resuspended in buffer A, and sonicated until a homogeneous solution was obtained. Aliquots were added to AChR-rich membrane suspensions 30 min before the fluorescent measurements. Buffer A was added to the control samples to measure dilution effects.

Fluorescence Measurements. All fluorimetric measurements were performed in a SLM model 4800 fluorimeter (SLM Instruments, Urbana, IL) using the vertically polarized light beam from a Hannovia 200 W Hg/Xe arc obtained with a Glan-Thompson polarizer (4 nm excitation and emission slits) and 10 × 10 mm quartz cuvettes. Emission spectra were corrected for wavelength-dependent distortions. The temperature was set at 20 °C with a thermostated circulating water bath.

(a) Laurdan Measurements. Laurdan was added to AChR-rich membrane samples from an ethanol solution to give a final probe concentration of 0.6 μM. The amount of organic solvent in these and all other experiments was kept below 0.2%. The samples were incubated in the dark for 60 min at room temperature. Excitation GP (*11, 12*) was calculated according to

$$\mathrm{exGP} = (I_{434} - I_{490})/(I_{434} + I_{490}) \qquad (1)$$

where I_{434} and I_{490} are the emission intensities at the characteristic wavelength of the gel phase (434 nm) and the liquid-crystalline phase (490 nm), respectively. exGP values were obtained from emission spectra at different excitation wavelengths (320−410 nm) or at only one excitation wavelength where indicated. Emission GP was calculated according to the following formalism:

$$\mathrm{emGP} = (I_{410} - I_{340})/(I_{410} + I_{340}) \qquad (2)$$

where I_{410} and I_{340} are the excitation intensities at the wavelengths corresponding to the gel (410 nm) and the liquid-crystalline (340 nm) phases, respectively (*20*). The emGP values were obtained from excitation spectra at different emission wavelengths (420−500 nm).

(b) Parallax Method. Solutions of spin-labeled phosphatidylcholines (SLPC) having different nitroxide spin-labeled acyl chains were made in ethanol, added to AChR-rich membrane samples previously labeled with Laurdan, and incubated for 20 min. A wavelength of 360 nm was used for direct excitation of Laurdan. The emission intensity of Laurdan (434 nm) in the presence and absence of the quencher was analyzed by using (*15*)

$$Z_{cF} = L_{c1} + \{[(-1/\pi C) \ln (F_1/F_2) - L_{21}^2]/2L_{21}\} \quad (3)$$

where Z_{cF} is the distance of the fluorophore from the center of the bilayer, L_{c1} is the distance between the center of the bilayer and the shallow quencher, 1; L_{21} is the distance between the two quenchers, C is the quencher concentration in molecules per unit area, and F_1 and F_2 are the fluorescence intensities in the presence of the shallow and deeper quenchers, respectively.

(c) Measurement of Steady-State Anisotropy of DPH and Its Derivatives. Aliquots of TMA-DPH or PA-DPH in tetrahydrofuran or DPH in dimethyl sulfoxide were added to the AChR-rich membrane suspension to give a final concentration of 1 μM. Samples were incubated at 25 °C for 30 min. The amount of organic solvent added was kept below 0.05%. The excitation and emission wavelengths used were 365 and 425 nm, respectively. Fluorescence anisotropy measurements were done in the T format with Schott KV418 filters in the emission channels and corrected for optical inaccuracies and for background signals. The anisotropy value, r_s, was obtained from eq 4 (see, e.g., ref *21*):

$$r_s = (I_v/I_h)_v - (I_v/I_h)_h \quad (4)$$
$$(I_v/I_h)_v + 2(I_v/I_h)_h$$

where $(I_v/I_h)_v$ and $(I_v/I_h)_h$ are the ratios of the emitted vertical or horizontally polarized light to the exciting, vertical or horizontally polarized light, respectively. r_s values can range between −0.2 and 0.4, the higher values denoting the higher structural lipid order.

(d) Förster Resonance Energy Transfer (FRET) Measurements. Measurements of the extent of quenching of donor fluorescence by Förster energy transfer were carried out in the absence and presence of increasing concentrations of Laurdan as in Antollini et al. (*13*). The energy transfer efficiency (E) in relation to all other deactivation processes of the excited donor depends on the sixth power of the distance between donor and acceptor. According to Förster's theory (*22*), E is given by

$$E = R_0^6/(R_0^6 + r^6) \quad (5)$$

where r is the intermolecular distance and R_0 is a constant parameter for each donor−acceptor pair, defined as the distance at which E is 50%. E can also be calculated as

$$E = 1 - (\phi/\phi_D) \approx 1 - (I/I_D) \quad (6)$$

where ϕ and ϕ_D are the fluorescence quantum yields of donor in the presence and absence of the acceptor, respectively; and I and I_D are the corresponding emission intensities in any given measurement. Here I and I_D correspond to the maximal intrinsic protein emission intensity, which is 330 nm.

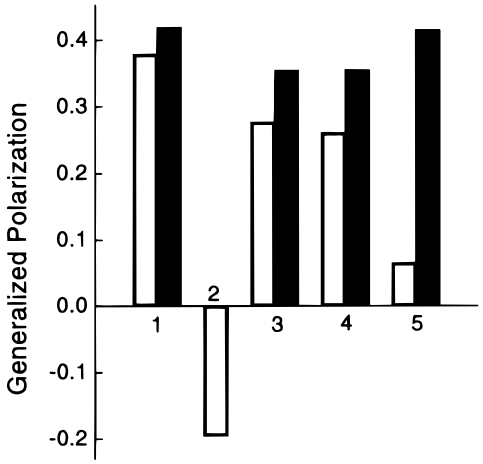

FIGURE 1: Laurdan excitation GP using direct excitation of the probe (360 nm, empty bars) or FRET (290 nm, filled bars) recorded under the following experimental conditions: (1) *T. marmorata* membranes labeled with Laurdan; (2) DOPC multilamellar liposomes labeled with Laurdan; (3) *T. marmorata* membranes labeled with Laurdan and supplemented with DOPC liposomes; (4) *T. marmorata* membranes supplemented with DOPC liposomes and subsequent addition of Laurdan; and (5) two independent samples of *T. marmorata* membranes labeled with Laurdan and DOPC multilamellar liposomes labeled with Laurdan were rapidly mixed immediately before recording the Laurdan emission spectrum. The exGP was calculated using the emission wavelengths at 434 and 490 nm. The DOPC, Laurdan, and membrane protein final concentrations in the cuvette were 20 μM, 0.6 μM, and 50 μg/mL, respectively. The temperature was 20 °C.

Control Laurdan GP Measurements in the Presence of Exogenous DOPC. To exclude the possibility that Laurdan molecules redistributed into the added liposomes in the time course of the titration, several control experiments were undertaken. The existence of large differences between the GP value of Laurdan in membranes and in DOPC liposomes (in the liquid-crystalline phase at 20 °C) was exploited when testing this issue. If the probe were to redistribute from the native membrane to the added liposomes, Laurdan GP would decrease significantly. We measured Laurdan GP using either direct excitation of the probe or under FRET conditions, under five different experimental situations (Figure 1): (1) *T. marmorata* membranes (50 μg of protein/mL) labeled with Laurdan (0.6 μM). (2) DOPC multilamellar liposomes labeled with Laurdan. In this case, DOPC and Laurdan in ethanol were evaporated under N_2, resuspended in buffer A, and sonicated until clarity to give final concentrations of 20 and 0.6 μM in the measuring cuvette, respectively. (3) *T. marmorata* membranes (50 μg of protein/mL) labeled with Laurdan (0.6 μM) and supplemented with DOPC liposomes (the final concentration in the cuvette was 20 μM). (4) *T. marmorata* membranes (50 μg of protein/mL) supplemented with DOPC liposomes (final concentration in the cuvette, 20 μM) and subsequently supplemented with Laurdan (0.6 μM). (5) Two independent samples of *T. marmorata* membranes (50 μg of protein/mL) labeled with Laurdan (0.3 μM) and DOPC multilamellar liposomes labeled with Laurdan, prepared as in condition 2 above (final concentration in the cuvette 20 and 0.3 μM, respectively) were rapidly mixed (the final concentration of Laurdan was

0.6 μM) immediately before recording the Laurdan emission spectrum.

As can be seen in Figure 1, Laurdan GP values were markedly different for AChR-rich membranes (GP ~0.38) and, interestingly enough, negative (−0.2) for DOPC liposomes. Furthermore, conditions 3 and 4 exhibited practically the same GP values. These results imply that either Laurdan molecules redistribute between native membranes and liposomes or that DOPC is effectively incorporated into *T. marmorata* native membrane. Experimental condition 5 was designed to discriminate between these two hypotheses. The GP value obtained by direct excitation of the probe in the mixture was smaller than the one obtained for conditions 3 and 4, whereas the GP value obtained under FRET conditions was similar to the GP value of situation 1 (i.e., in the absence of DOPC). From this, we conclude that under our experimental conditions there is considerable incorporation of DOPC into *T. marmorata* membranes, thus excluding the possibility that Laurdan molecules redistribute significantly between the native AChR-rich membrane and added lipid vesicles (if such redistribution had taken place, the GP values would have been much lower for conditions 3 and 4).

RESULTS

Modifications in the Solvent Dipolar Relaxation and in the Polarity of the AChR Membrane Induced by Exogenous lipids. The AChR interacts preferentially with distinct lipid species such as sterols, negatively charged phospholipids, and fatty acids (*3*, *4*, *23*, *24*). We investigated the possible modification of the polarity of both the AChR belt and bulk lipid regions by oleic acid, DOPC, and CHS, respectively. In a first series of experiments Laurdan was incorporated into the AChR-rich membrane and excited directly at 360 nm or under FRET conditions at 290 nm. Laurdan GP was calculated by the following algorithm (*10*):

$$\mathrm{GP} = (I_B - I_R)/(I_B + I_R) \qquad (7)$$

where I_B (434 nm) and I_R (490 nm) are the fluorescence intensities at the blue and red edges of the emission spectrum, respectively. We have previously shown that GP values observed under energy transfer conditions from the intrinsic protein fluorescence in AChR membrane from *T. marmorata* exhibit higher absolute GP values than those obtained by direct excitation of the probe, indicating the lower polarity of the lipid in the microenvironment of the AChR protein (*13*).

As shown in Figure 2a, GP values decreased with increasing 18:1 concentrations, indicating an augmentation in the solvent dipolar relaxation and in the polarity (*12*) of the membrane regions where Laurdan is located. Furthermore, the slopes of the curves displayed by the GP values in the presence of 18:1 using either direct excitation or FRET conditions were almost identical. This indicates that oleic acid partitions well into belt and bulk lipid and that the change in membrane polarity brought about by the fatty acid is similar in the two operationally defined lipid regions. GP values also decreased upon enrichment of the AChR membrane with DOPC (Figure 2b). Since the slopes of the experimental values were similar under the two sets of conditions, as observed with oleic acid, one can infer that there was no preference of DOPC for either the belt or bulk lipid regions. In fact, PC exhibits no selectivity for the AChR (*23*).

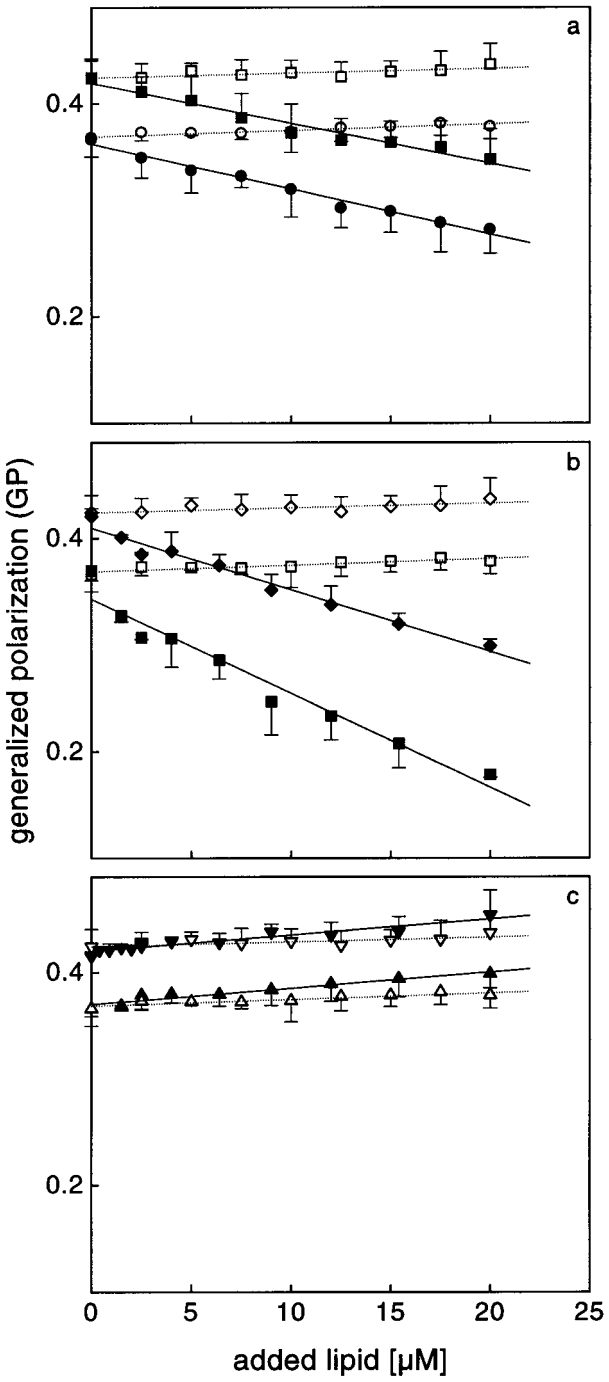

FIGURE 2: Laurdan excitation GP using direct excitation of the probe (360 nm) or FRET (290 nm) from the protein emission in *T. marmorata* AChR membrane (a) in the presence and absence of increasing concentrations of oleic acid (●,○, 360 nm; ■, □, 290 nm), respectively; (b) in the presence and absence of increasing concentrations of DOPC (■,□, 360 nm; ♦, ◊, 290 nm), respectively; and (c) in the presence and absence of increasing concentrations of CHS using direct excitation at 360 nm (▲,△) or 290 nm (▽,▼). GP was calculated using the emission wavelengths at 434 and 490 nm. The Laurdan to membrane lipid ratio was 1:100. Each point corresponds to the average ± standard deviation of three determinations. Experiments in this and all other figures were carried out at 20 °C.

We also studied the effect of cholesterol enrichment of the AChR membrane. Instead of using cholesterol, we prefer to use CHS, a water-soluble ester of cholesterol, since the

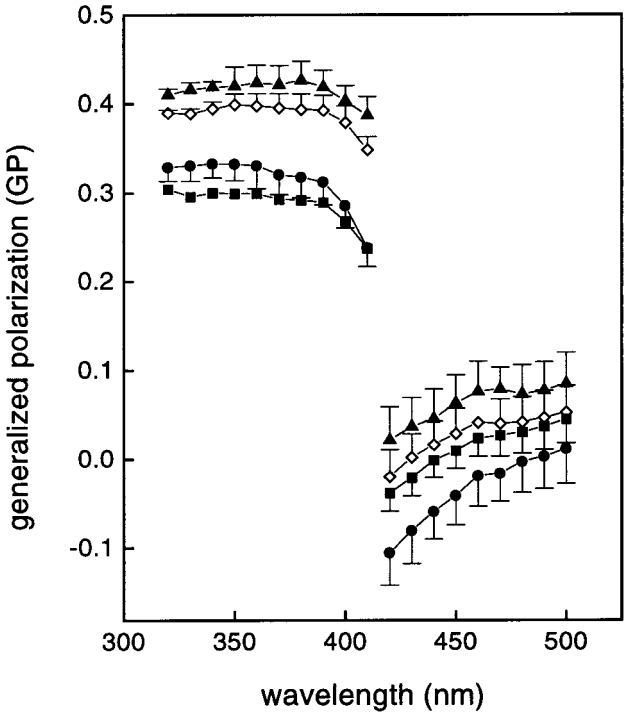

FIGURE 3: Laurdan GP in the *T. marmorata* AChR membrane as a function of excitation (320−410 nm) and emission (420−500 nm) wavelengths in the absence (◊) and presence of 10 μM oleic acid (●), 10 μM DOPC (■,) and 10 μM CHS (▲). Values of emission at 434 and 490 nm were used for recording the excitation spectra, and maxima at 340 and 410 nm were measured for the emission spectra, respectively. The Laurdan to membrane lipid ratio was 1:100. Each point corresponds to the average ± standard deviation of three determinations.

low aqueous solubility of the former makes it difficult to modify the cholesterol content of samples such as the native AChR membrane in which this neutral lipid is particularly abundant (*6*). Simmonds et al. (*25*) characterized the interactions of CHS with phospholipids, concluding that CHS can be used to directly modify the sterol content of membranes without the use of detergents; their results with CHS were very similar to those obtained with cholesterol. In the present work, addition of CHS to native *T. marmorata* AChR membrane produced only a slight, statistically non-significant increase in GP values (Figure 2c). The slopes of the experimental values obtained under direct excitation or FRET conditions were similar, implying no preferential partition of the cholesterol derivative into either belt or bulk lipid regions, as already commented in the cases of oleic acid and DOPC.

Exogenous Lipids Do Not Induce Phase Separation in the AChR-Rich Membrane. Further information about the environment of the reporter Laurdan molecules could be obtained from the wavelength dependence of GP spectra (*20*). A wavelength-independent GP spectrum is characteristic of the gel phase, whereas in liquid-crystalline phases GP typically exhibits wavelength dependence, due to solvent dipolar relaxation, with decreasing values for the excitation GP spectrum and increasing values for the emission GP spectrum.

We studied GP in native *T. marmorata* AChR membrane as a function of excitation (320−410 nm) and emission (420−500 nm) wavelengths at 20 °C in the presence and absence of 18:1, DOPC, and CHS (Figure 3). Excitation and emission GP values were calculated according to eqs 1 and 2. Lower GP values were observed upon the addition of oleic acid or DOPC and higher values in the case of CHS. The spectra exhibited in all cases decreasing values of exGP and increasing values of emGP with increasing wavelength (Figure 3).

This behavior indicates that solvent dipolar relaxation remains unchanged in the presence of exogenous lipids and that there is no selective excitation of subpopulations of Laurdan molecules, thus suggesting that the Laurdan microenvironment in the presence of these different exogenous lipids maintains the characteristics of the native AChR-rich membrane, i.e., an ordered liquid phase (*13*). The effect of exogenous lipid would therefore appear to be exerted on the whole membrane lipid, without inducing the formation of separate microdomains.

Modifications of the Membrane Lipid Order of Each Leaflet in the AChR Membrane by Exogenous Lipids. To further explore the effect of the different exogenous lipids on the physical state of the AChR membrane, the steady-state anisotropy at different depths across the membrane was investigated in a second series of complementary experiments using three well-known fluidity-sensitive probes: DPH and two derivatives, PA-DPH and TMA-DPH (Figure 4). Increasingly lower DPH anisotropy values were observed upon increasing the concentration of 18:1, indicating a decrease in the order of the membrane phospholipid acyl chains (Figure 4, panels a and d). A similar decrease was observed in the fluorescence anisotropy of the two DPH analogues (Figure 4), albeit of smaller magnitude than that observed with DPH. This implies that the increase in the fluidity of the AChR membrane sensed by PA- and TMA-DPH at more superficial levels of the membrane as a function of oleic acid is less marked than that occurring deeper in the hydrocarbon core of the membrane.

Addition of increasing amounts of DOPC induced a decrease in the anisotropy values of DPH and of its polar derivative PA-DPH, whereas very little if any effect was observed with TMA-DPH, the cationic derivative (Figure 4, panels b and e). Thus, the addition of exogenous DOPC to the AChR membrane seems to induce modification of the exofacial hemilayer and of the core of the membrane with little if any changes in the cytoplasmic hemilayer. Increasing amounts of CHS (Figure 4, panels c and f) did not modify the anisotropy values of DPH and PA-DPH, the DPH derivative sensing the exofacial hemilayer, whereas a decrease of the anisotropy values of the TMA-DPH, the cytofacial hemilayer-sensing probe, was obtained.

Topography of Laurdan Site in Native T. marmorata AChR Membrane. The parallax method described by Chattopadhyay and London (*15*) was used to determine the average depth of Laurdan in the native AChR membrane. This method is based on the relative position of a fluorescence probe embedded in the membrane and spin label quenchers having nitroxide spin labels at different vertical positions along their acyl chains. This is accomplished by pairwise comparison of quenching parameters with different probes. Chattopadhyay and McNamee (*26*) applied this method to reconstituted *T. californica* AChR to calculate the distance of γ-subunit Trp453 from the bilayer center, obtaining an average value of ∼10 Å. In the present work, the topography of Laurdan in native *T. marmorata* AChR-rich membranes

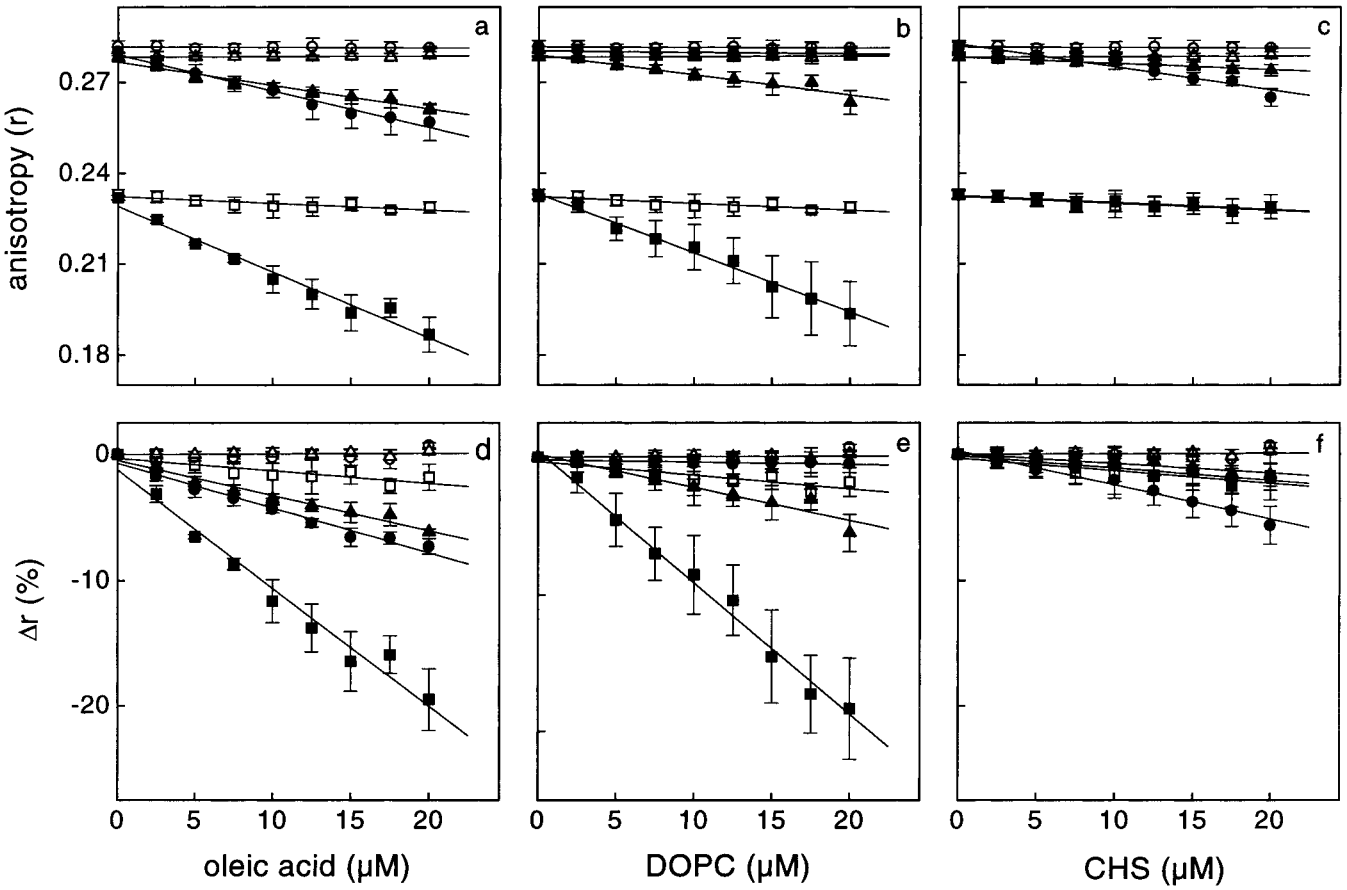

FIGURE 4: Panels a−c show the fluorescence anisotropy (*r*) of DPH (■), TMA-DPH (●), and PA-DPH (▲) in *T. marmorata* AChR membrane as a function of (a) oleic acid, (b) DOPC, and (c) CHS. Panels d−f depict the relative changes in fluorescence anisotropy (Δ*r*) of DPH (■), TMA-DPH (●), and PA-DPH (▲) as a function of (d) oleic acid, (e) DOPC, and (f) CHS. Empty symbols are control samples in the absence of exogenous lipid. The probe to membrane lipid ratio was kept at 1:100 in all cases. Each point corresponds to the average ± standard deviation of three determinations.

Table 1: Average Depth of Laurdan in Native *T. marmorata* AChR-Rich Membrane[a]

spin-labeled PC pair	Z_{CF} (Å)[a]	av. Z_{CF} (Å)
7-PC/12-PC	11.0	
7-PC/10-PC	10.0	9.8
10-PC/12-PC	8.3	

[a] Measured by the parallax method (*15*). Each measurement stems from three independent series of experiments. An average distance (Z_{CF}) with a variation of less than 2% was calculated.

was determined from the quenching data obtained with pairwise combinations of the PC analogues 7-SLPC, 10-SLPC, and 12-SLPC (eq 3 and Figure 5). Maximal quenching of Laurdan emission was obtained with the quencher having the shallower location, 7-SLPC.

Given the dimensions of Laurdan's molecule (*27, 28*) and the thickness of the *Torpedo* AChR membrane hydrocarbon region of ∼30 Å (*29, 30*), an average depth (Z_{cF}) of ≈9.8 Å could be obtained from the data in Figure 5 (see Table 1). This implies that Laurdan's dimethylamino group is at a shallower position in the polar/hydrocarbon interface, at ∼5 Å from the membrane surface, whereas its acyl tail penetrates deeper in the hydrocarbon region, being located at ∼10 Å from the center of the bilayer. An average value is obtained because of the distribution of depths of fluorophores and spin labels, respectively. This value can fluctuate between a couple of angstroms (*15*). Laurdan GP (see Materials and Methods) was calculated for each addition of quencher. Figure 5 inset shows that no significant differences were apparent in Laurdan GP values at any of the concentrations used.

Discrete Binding Sites for Different Lipids in the AChR−Lipid Interface Region. Jones and McNamee (*4*) postulated the occurrence of two different classes of lipid sites, annular and non-annular, in purified, reconstituted AChR, as previously suggested by Simmonds et al. (*25*) for Ca^{2+},Mg^{2+}-ATPase. Some phospholipids are reported to display moderate selectivity for the annular region, whereas cholesterol is preferentially partitioned in the non-annular region; fatty acids are found in both regions. Since Laurdan is a fatty acid derivative, one would expect it to partition in both regions. Taking advantage of the photoselection resulting from energy transfer conditions, Laurdan molecules in the AChR lipid microenvironment are expected to emit upon excitation of the donor Trp residues in the 290 nm region. Figure 6 shows the decrease in the efficiency of the energy transfer process, *E*, in the presence of increasing amounts of exogenous lipids.

The maximal decrease in *E* resulting from the addition of 18:1 amounted to about 60%. Further addition of either CHS or DOPC produced a diminution in *E* of 35% and 25%, respectively. The sum of the decreases caused by DOPC and CHS equaled that obtained in the presence of 18:1 alone (Figure 6). This suggests (a) the occurrence of different sites for DOPC and CHS and (b) that both sets of sites are also accessible to oleic acid.

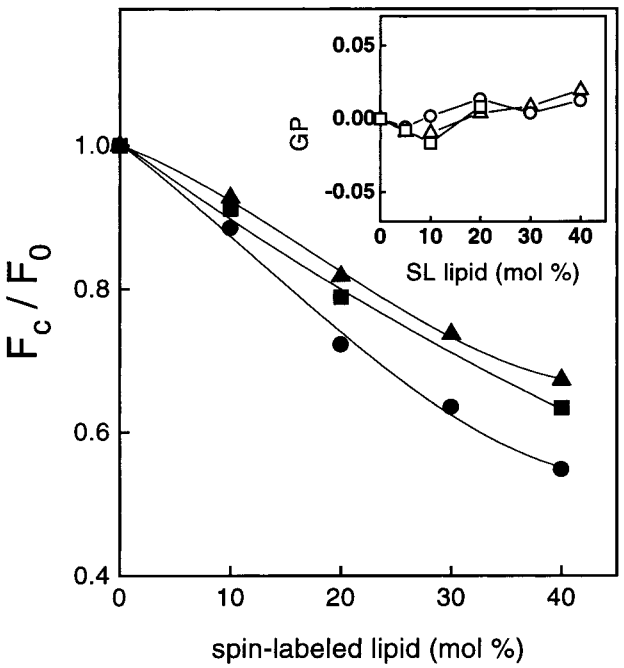

FIGURE 5: Quenching of Laurdan fluorescence in *T. marmorata* AChR membrane by 7-doxyl-PC (●), 10-doxyl-PC (■,) and 12-doxyl-PC (▲) spin label analogues. F_c and F_0 are the fluorescence emission intensities of Laurdan measured at 434 nm and corrected for dilution and lamp distortions, in the presence and absence of the nitroxide spin label, respectively. Inset: Lack of dependence of GP on the PC spin label concentration.

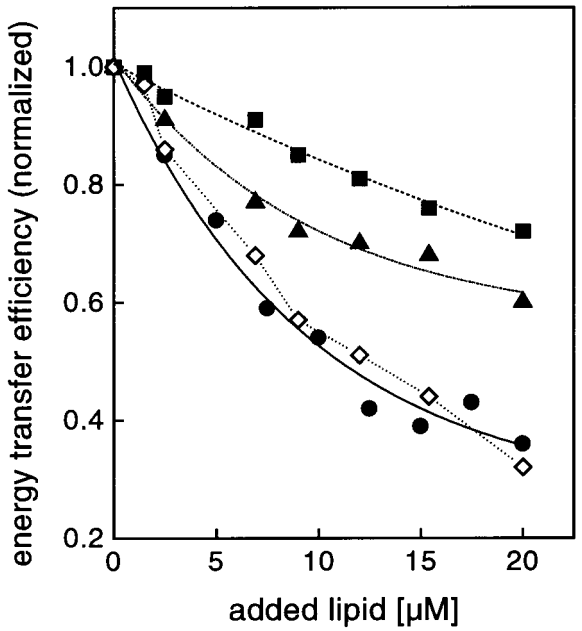

FIGURE 6: Normalized energy transfer efficiency, *E*, between AChR in native *T. marmorata* membrane and Laurdan in the presence of increasing concentrations of DOPC (■), CHS (▲), and oleic acid (●). (◊) Correspond to the sum of *E* of DOPC and CHS. Each point corresponds to the average ± standard deviation of four determinations.

To corroborate that the two sites were different, we conducted an additional series of experiments using the following strategy: First, we saturated one site with either CHS or DOPC (Figure 7) and then added the second lipid to see whether the decrease in *E* caused by the two was additive. When CHS was added first, *E* decreased by about 35%. Subsequent addition of DOPC or 18:1 caused a further

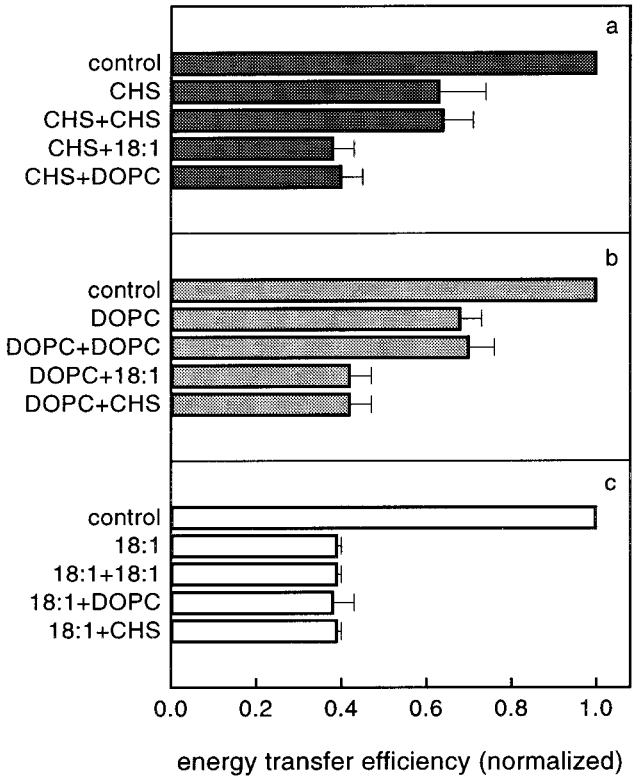

FIGURE 7: Normalized energy transfer efficiency, *E*, for the AChR/Laurdan pair in *T. marmorata* membranes. Three different conditions were carried out for each series of experiments, starting in all cases with AChR-rich membrane in the presence of 0.6 μM Laurdan, and then with (a) 20 μM CHS (dark gray), (b) 20 μM DOPC (light gray), and (c) 20 μM oleic acid (empty bar). Subsequent additions of (a) 10 μM CHS, 10 μM oleic acid, and 10 μM DOPC were made (each experimental condition corresponds to a bar, from top to bottom). In panel b 10 μM DOPC, 10 μM oleic acid, and 10 μM CHS were added. In panel c 10 μM oleic acid, 10 μM DOPC, and 10 μM CHS were added, from top to bottom. Each bar corresponds to the average ± standard deviation of four independent experiments.

reduction of *E* of ∼25%, the total effect thus amounting to ∼60% (Figure 7a). Analogously, when DOPC was used first, the initial decrease amounted to ∼25%, and subsequent additions of 18:1 and DOPC yielded a total diminution of *E* of about 60% (Figure 7b). When oleic acid was added first, an initial reduction of ∼60% was obtained, and subsequent additions of CHS and DOPC attained similar levels of *E* (Figure 7c). Thus, Laurdan displacement by CHS or DOPC is *independent* and *additive*, while oleic acid alone caused a displacement equivalent to the *combined* effects of DOPC and CHS. From these experiments, it can be postulated that sites for phospholipid and sterol, both accessible to fatty acid, are distinct.

DISCUSSION

In the present work, we used various fluorescence techniques to study the physical properties of the native *Torpedo* AChR membrane and to determine whether exogenous lipids modify such properties. Laurdan GP and the fluorescence anisotropy of DPH and its derivatives PA-DPH and TMA-DPH provided complementary information on the bulk physical state of the membrane such as lipid packing order across the exofacial, the cytoplasmic facing, and the hydrocarbon regions of the AChR membrane. FRET was used to

discriminate between the bulk lipid and the belt lipid region in the vicinity of the protein. Further refinement of this topographical information was provided by the parallax method using phospholipid spin labels. Finally, changes in energy transfer efficiency induced by fatty acids, phospholipid, and cholesterol led to the identification of discrete sites for these lipids on the AChR protein.

Laurdan localizes itself at the lipid−water interface of the bilayer with its naphthalene group at the phospholipid polar headgroup region and its 12-C lauric acid tail immersed in the phospholipid acyl chain region and is considered to have uniform lateral and transbilayer distribution, thus making it a good reporter molecule to sense molecular dynamics of solvent dipoles in the membrane as a whole. We have shown that Laurdan does not have selectivity for either belt or bulk lipid regions in the AChR membrane (*13*). The good spectral overlap between AChR and Laurdan and the decrease in protein emission observed in the presence of Laurdan correlated with the increase in Laurdan emission intensity were exploited in our FRET studies. To use FRET conditions to characterize discrete sites for lipids at the protein−lipid interface, it is necessary to know the relative position of the donor and acceptor molecules. In a previous work, taking advantage of an analytical approach developed by Gutierrez-Merino et al. (*31, 32*), a minimum donor−acceptor distance of 14 ± 1 Å could be calculated for the Laurdan−AChR pair in the *T. marmorata* native membrane (*13*), in agreement with the postulated location of Laurdan in other membranes (*11, 27, 28*) and with the overall dimensions of the AChR and its transmembrane region in particular (*30*). Here we used the parallax method developed by Chattopadhyay and London (*15*) to obtain the position of Laurdan relative to the AChR membrane bilayer (Figure 5). Maximal quenching of the Laurdan emission was obtained with the shallower quencher, 7-SLPC. A value of ∼10 Å was obtained for the distance of Laurdan from the center of the bilayer. The AChR has 51 Trp residues but only one in its membrane-spanning region (Trp-453 in the γ-subunit M4 domain). Using the parallax method, Chattopadhyay and McNamee (*26*) found that Trp-453 was at about 10 Å from the bilayer center in AChR membrane. Thus, Laurdan and Trp-453 are located almost at the same plane parallel to the bilayer surface. This is in agreement with earlier work from our laboratory in which the relative position of membrane-embedded AChR tryptophan residues at the apolar−polar interface was inferred from quenching of membrane-bound AChR with spin-labeled fatty acids (*33*).

Laurdan GP values depend on the polarity and dynamics of the dipoles in the environment of the probe. The main dipoles sensed by Laurdan in the membrane are water molecules. When no relaxation occurs, high GP values result, indicative of low water content in the hydrophilic/hydrophobic interface region of the membrane. Differences in GP values have been correlated with variations in membrane lipid fluidity (*34*) whereas fluorescence anisotropy of DPH and its derivatives provides information on the orientational order of lipids in the membrane. Kleinfeld et al. (*35*) and Pottel et al. (*36*) established that DPH steady-state fluorescence anisotropy could be correlated with packing-sensitive motional modes of the membrane lipid rather than measure membrane microviscosity. Thus, the two types of fluorescence compounds used in the present work—Laurdan and DPH and derivatives—yield topographically distinct yet complementary information. The shallow localization of Laurdan molecules provides average information on the physical state of both hemilayers, whereas DPH and its derivatives PA- and TMA-DPH report on the acyl chain packing order of the inner hydrocarbon core, the exofacial- and the cytoplasmic-facing acyl chain regions, respectively.

Patch-clamp single-channel recordings show that fatty acids shorten the AChR open dwell-time (*37*). Phospholipids containing short-chain fatty acids induce a decrease in the frequency of AChR channel openings (*38*). It was therefore of interest to investigate whether the changes in AChR function induced by fatty acids could be correlated with changes in the physical properties of the lipid in the membrane. Indeed, oleic acid (18:1) and dioleoyl-PC increased the polarity of both bulk and belt lipid regions in the native AChR membrane (Figure 2). No phase separation was induced by these lipids since no selective excitation of subpopulations of Laurdan molecules was observed in either case (Figure 3). CHS did not induce a statistically significant change in GP (Figure 2). *T. marmorata* AChR membrane is highly enriched in cholesterol (*6, 39*); therefore, additional cholesterol can be expected to produce little if any change. From the wavelength dependence of Laurdan GP, we could further ascertain that no phase separation occurs upon addition of CHS (Figure 3).

In many biological membranes, the two hemilayers differ in lipid composition and fluidity. The outer monolayer of synaptic plasma membranes is more fluid than the inner leaflet (*40, 41*). This difference in fluidity between the two leaflets of the membrane has been reported to amount to a 6% change in temperature or to the effect of 400 mM ethanol in vitro (*42*). In rat myotubes, the regions of the membrane where AChRs occur in clusters exhibit phospholipid asymmetry (*43*); at least 77% of the plasma membrane aminophospholipids, phosphatidylserine and phosphatidylethanolamine associated with the clusters were found to be located in the inner, cytoplasmic leaflet of the membrane. In the particular case of the *T. marmorata* AChR-rich membrane, we have shown that in addition to the asymmetrical disposition of lipids between bulk and lipid belt regions, the topological distribution of the principal phospholipid components between the two hemilayers is also asymmetrical and that this difference results in an electrostatic membrane potential of ∼15 mV (*17, 44*). These findings are not surprising, given the asymmetrical transmembrane distribution of the AChR protein itself as judged from electron microscope data (*30*). So far, however, no attempts have been made to analyze the fluidity of the lipid across the AChR membrane.

DPH localizes itself at the hydrocarbon core of the bilayer, aligned parallel the phospholipid acyl chains (*45*), and is a well-established reporter group of the bulk order or fluidity of the membrane. The cationic derivative trimethylaminodiphenylhexatriene (TMA-DPH) preferentially partitions in the inner, cytoplasmic hemilayer, and the anionic derivative propionic acid (PA-DPH) does so in the outer, exofacial leaflet (*46, 47*). Lipid packing order imposes restrictions on the rotational motion of the acyl chains. In native *T. marmorata* AChR membrane, the center of the bilayer appears to be the most fluid, disordered region, as sensed

by DPH, in comparison to the more superficial, polar headgroup regions sensed by TMA-DPH and PA-DPH (Figure 4). Addition of oleic acid further increased the disorder in the membrane lipid, mainly at the hydrocarbon core. This is in accordance with Berlin et al. (*48*), who studied the effect of fatty acids on the membrane fluidity of the CHO cell line TR715-19. They reported that fatty acids modified mid-bilayer fluidity, determined with DPH, but fluidity in the polar phospholipid headgroup regions, sensed with PA-DPH and TMA-DPH, was independent of fatty acid composition.

DOPC also caused the diminution of the lipid order in the AChR membrane, but at variance with oleic acid, the changes extended from the hydrocarbon central region to the shallower headgroup region of the outer hemilayer (Figure 4). Studies with model membranes provide clear evidence that the transbilayer movement of phospholipids is an extremely slow, almost negligible process (a $t_{1/2}$ of 11−15 days was calculated for radiolabeled PC in small unilamellar vesicles; *49*). PC flip-flop is an unlikely process in the time scale of our measurements, thus explaining the observation of the disordering effect in the exofacial hemilayer only.

The slight disordering effect of CHS was only apparent in the very modest decrease of TMA-DPH fluorescence anisotropy, thus reflecting the selective changes at the polar headgroup region of the inner hemilayer (Figure 4). That these changes were not sensed by Laurdan GP (Figure 2) can be explained by the fact that this probe averages GP contributions of both hemilayers. Cholesterol and derivatives generally increase the membrane lipid order, unless the system is already ordered, in which case cholesterol exerts a disordering effect. Native *T. marmorata* AChR membrane has large amounts of cholesterol and may fall in this latter category. Contrary to what is observed with polar lipids, the transbilayer movement of nonpolar lipids such as cholesterol appears to be rapid in model systems ($t_{1/2}$ of 1 min or less; *49*). If this is the case with the AChR membrane, our results might indicate some degree of selectivity of CHS for the inner hemilayer, an issue that deserves further investigation.

Three classes of lipid (fatty acid, phospholipid, and sterol) displace Laurdan from the AChR lipid microenvironment. Such displacements are independent of one another and additive, while the effect caused by fatty acid alone amounts to the sum of the effects caused by DOPC and CHS together (Figures 6 and 7). Thus two classes of lipid sites appear to occur in the native *T. marmorata* AChR membrane, one for phospholipid (and not sterol) and the other for sterol (and not phospholipid), both accessible to fatty acid. These sites may be equivalent to the annular and non-annular sites characterized by Jones and McNamee (*4*) and Narayanaswami and McNamee (*50*). The latter authors used AChR covalently labeled with *N*-(1-pyrenyl)maleimide and brominated lipids as quenchers. When the quencher was diBr-CHS they obtained an effective quenching of ∼35%, and when the quencher was 6,7-BrPC, an effective quenching of ∼25% was obtained. Although the two strategies differ, it is interesting to note that the extent of quenching reported by these authors and the percentage decrease of *E* in the present work are identical. In the present work, the effect of 18:1 equaled that of the sum of the two other lipids. From this, we infer that the fatty acid competes for both sites. In Narayanaswami and McNamee's work (*50*), brominated stearic acid (6,7-diBrStA) did not equal the effect of the two others lipids together (<5% quenching in addition to the 25% produced by 6,7-BrPC). The main difference between the two series of experiments is that Narayanaswami and McNamee (*50*) used *T. californica* AChR reconstituted in pure DOPC, whereas in the present work native *T. marmorata* AChR-rich membrane is used. Further experiments are needed to elucidate this point and to determine the stoichiometry of these sites.

In conclusion, oleic acid, DOPC, and CHS effectively partition into the bulk lipid and the AChR lipid microenvironment changing the polarity and packing order without leading to the formation of microdomains. In a previous work, we characterized the AChR−Laurdan pair as a donor−acceptor couple for Förster-type energy transfer measurements. Here we introduce a novel strategy, using the efficiency of this process to measure displacement of Laurdan from the AChR lipid microenvironment caused by exogenous lipids, and in this way to characterize sites for these lipids in the vicinity of the protein. Using this approach, the occurrence of discrete and independent classes of lipid sites for sterol and phospholipid are disclosed in the native AChR-rich membrane. Future studies will be aimed at determining the exact stoichiometry of these sites and their functional regulation.

REFERENCES

1. Barrantes, F. J. (1989) *Crit. Rev. Biochem. Mol. Biol. 24*, 437−478.
2. Barrantes, F. J. (1993) *FASEB J. 7*, 1460−1467.
3. Marsh, D., and Barrantes, F. J. (1978) *Proc. Natl. Acad. Sci. U.S.A. 75*, 4329−4333.
4. Jones, O. T., and McNamee, M. G. (1988) *Biochemistry 27*, 2364−2374.
5. East, J. M., Jones, O. T., Simmonds, A. C., and Lee, A. G. (1984) *J. Biol. Chem. 259*, 8070−8071.
6. Criado, M., Vaz, W. L. C., Barrantes, F. J., and Jovin, T. M. (1982) *Biochemistry 21*, 5750−5755.
7. Criado, M., Eibl, H., and Barrantes, F. J. (1984) *J. Biol. Chem. 259*, 9188−9198.
8. Fong, T. M., and McNamee, M. G. (1986) *Biochemistry 25*, 830−840.
9. Sunshine, C., and McNamee, M. G. (1994) *Biochim. Biophys. Acta 1191*, 59−64.
10. Parasassi, T., Conti, F., and Gratton, E. (1986) *Cell. Mol. Biol. 32*, 103−108.
11. Parasassi, T., De Stasio, G., d'Ubaldo, A., and Gratton, E. (1990) *Biophys. J. 57*, 1179−1186.
12. Parasassi, T., De Stasio, G., Ravagnan, G. Rusch, R., and Gratton, E. (1991) *Biophys. J. 60*, 179−189.
13. Antollini, S. S., Soto, M. A., Bonini de Romanelli, I., Gutiérrez Merino, C., Sotomayor, P., and Barrantes, F. J. (1996) *Biophys. J. 70*, 1275−1284.
14. Zanello, L. P., Aztiria, E., Antollini, S., and Barrantes, F. J. (1996) *Biophys. J. 70*, 2155−2164.
15. Chattopadhyay, A., and London, E. (1987) *Biochemistry 26*, 39−45.
16. Barrantes, F. J. (1982) In *Neuroreceptors* (Hucho, F., Ed.) pp 315−328, Walter de Gruyter, Berlin, New York.
17. Gutiérrez-Merino, C., Pietrasanta, L., Bonini de Romanelli, I., and Barrantes, F. J. (1995) *Biochemistry 34*, 4846−4855.
18. Richieri, G. V., Ogata, R. T., and Kleinfeld, A. M. (1992) *J. Biol. Chem. 267*, 23495−23501.
19. Simpson, R. B., Ashbrook, J. D., Santos, E. C., and Spector, A. A. (1974) *J. Lipid Res. 13*, 415−422.

20. Parasassi, T., Loiero, M., Raimondi, M., Ravagnan, G., and Gratton, E. (1993) *Biochim. Biophys. Acta 1153*, 143−154.
21. Shinitzky, M., and Yuli, Y.(1982) *Chem. Phys. Lipids 30*, 261−282.
22. Förster, Th. (1948) *Ann. Phys. (Leipzig) 2*, 55−75.
23. Marsh, D., Watts, A., and Barrantes, F. J. (1981) *Biochim. Biophys. Acta 645*, 97−101.
24. Ellena, J. F., Blazing, M. A., and McNamee, M. G. (1983) *Biochemistry 22*, 5523−5535.
25. Simmonds A. C., Rooney, E. K., and Lee, A. G (1984) *Biochemistry 25*, 7535−7544.
26. Chattopadhyay, A., and McNamee, M. G. (1991) *Biochemistry 30*, 7159−7164.
27. Chong, P. L.-G. (1988) *Biochemistry 27*, 399−404.
28. Chong, P. L.-G. (1990) *High-Pressure Res. 5*, 761−763.
29. Klymkowsky, M., and Stroud, R. M. (1979) *J. Mol. Biol. 128*, 319−334.
30. Unwin, N. (1993) *J. Mol. Biol. 229*, 1101−1124.
31. Gutiérrez-Merino, C., Munkonge, F., Mata, A. M., East, J. M., Levinson, B. L., Napier, R. M., and Lee, A. G. (1987) *Biochim. Biophys. Acta 897*, 207−216.
32. Gutiérrez-Merino, C., Centeno, F., García-Martin, E., and Merino, J. M. (1994) *Biochem. Soc. Trans. 22*, 784−788.
33. Barrantes, F. J. (1978) *J. Mol. Biol. 124*, 1−16.
34. Yu, W., So, P. T., French, T., and Gratton, E. (1996) *Biophys. J. 70*, 626−636.
35. Kleinfeld, A. M., Dragsten, P., Klausner, R. D., Pjura, W. J., and Matayoshi, E. D. (1981) *Biochim. Biophys. Acta 649*, 471−480.
36. Pottel, H., Van der Meer, W., and Herreman, W. (1983) *Biochim. Biophys. Acta 730*, 181−186.
37. Bouzat, C. B., and Barrantes, F. J. (1993) *Recept. Channels 1*, 251−258.
38. Braun, M. S., and Haydon, D. A. (1991) *Pflugers Arch 418*, 62−67.
39. González-Ros, J. M., Llanillo, M., Paraschos, A., and Martinez-Carrion, M. (1982) *Biochemistry 21*, 3467−3474.
40. Schroeder, F., Morrison, W. J., Gorka, C., and Wood, W. G. (1988) *Biochim. Biophys. Acta 946*, 85−94.
41. Wood, W. G., Gorka, C., and Schroeder, F. (1989) *J. Neurochem. 52*, 1925−1930.
42. Igvabova, U., Avdulov, N. A., Schroeder, F., and Wood, W. G. (1996) *J. Neurochem. 66*, 1717−1725.
43. Scher, M. G., and Bloch, R. J. (1993) *Exp. Cell Res. 208*, 485−491.
44. Bonini de Romanelli, I. C., Aveldaño, M. I., and Barrantes, F. J. (1990) *Int. J. Biochem. 22*, 785−789.
45. Andrich, M. P., and Vanderkooi, J. M. (1976) *Biochemistry 15*, 1257−1261.
46. Kitagawa, S., Matsubayashi, M., Kotani, K., Usui, K., and Kametani, F. (1991) *J. Membr. Biol. 119*, 221−227.
47. Kuhry, J.-G., Fontenau, P., Duportail, G., Maechling, C., and Laustriat, G. (1983) *Cell Biophys. 5*, 129−140.
48. Berlin, E., Hannah, J. S., Yamane, K., Peters, R. C., and Howard, B. V. (1996) *Int. J. Biochem. Cell Biol. 28*, 1131−1139.
49. Voelker, D. R. (1991) In *Biochemistry of Lipids, Lipoproteins and Membranes* (Vance, D. E., and Vance, J., Eds.) pp 489−523, Elsevier, Amsterdam.
50. Narayanaswami, V., Kim, J., and McNamee, M. G. (1993) *Biochemistry 32*, 12420−12427.

BI9808215